

---

# Value Memory Graph: A Graph-Structured World Model for Offline Reinforcement Learning

---

Deyao Zhu<sup>1</sup> Li Erran Li<sup>2</sup> \*Mohamed Elhoseiny<sup>1</sup>

<sup>1</sup> King Abdullah University of Science and Technology

<sup>2</sup> AWS AI, Amazon and Columbia University

{deyao.zhu, mohamed.elhoseiny}@kaust.edu.sa erranlli@gmail.com

## Abstract

World models in model-based reinforcement learning usually face unrealistic long-time-horizon prediction issues due to compounding errors as the prediction errors accumulate over timesteps. Recent works in graph-structured world models improve the long-horizon reasoning ability via building a graph to represent the environment, but they are designed in a goal-conditioned setting and cannot guide the agent to maximize episode returns in a traditional reinforcement learning setting without externally given target states. To overcome this limitation, we design a graph-structured world model in offline reinforcement learning by building a directed-graph-based Markov decision process (MDP) with rewards allocated to each directed edge as an abstraction of the original continuous environment. As our world model has small and finite state/action spaces compared to the original environment, value iteration can be easily applied here to estimate state values on the graph and figure out the best future. Unlike previous graph-structured world models that requires externally provided targets, our world model, dubbed **Value Memory Graph** (VMG), can provide the desired targets with high values by itself. VMG can be used to guide low-level goal-conditioned policies that are trained via supervised learning to maximize episode returns. Experiments on the D4RL benchmark show that VMG can outperform state-of-the-art methods in several tasks where long horizon reasoning ability is crucial. Code will be made publicly available.

## 1 Introduction

World models help agents understand environment dynamics and improve policies in sample efficiency [16] and performance [35]. Many world models in model-based reinforcement learning are designed to regress the environment transition  $p(s_{t+1}, r_t | s_{:t}, a_{:t})$ . Therefore, to predict the long-horizon future, agents have to roll out the world model step by step combined with an exhaustive search in the action space. Due to the accumulation of the prediction error at each step, these future estimations can quickly diverge from reality [16, 43]. To address this problem, graph-structured world models [7, 43] in goal-conditioned reinforcement learning use previously seen data to build a memory graph and reason the future by searching on the graph to reach the given target. Predictions here keep close to reality as they are from retrieved memories experienced in the environment. Although they show promising results in goal-conditioned reinforcement learning, they focus on reaching given goal states instead of maximizing episode returns. Therefore, in traditional reward-guided reinforcement learning tasks where the “goal state” is not given, these graph-structured world models don’t know which future states they should go to maximize received rewards.

---

\*Work done outside of Amazon

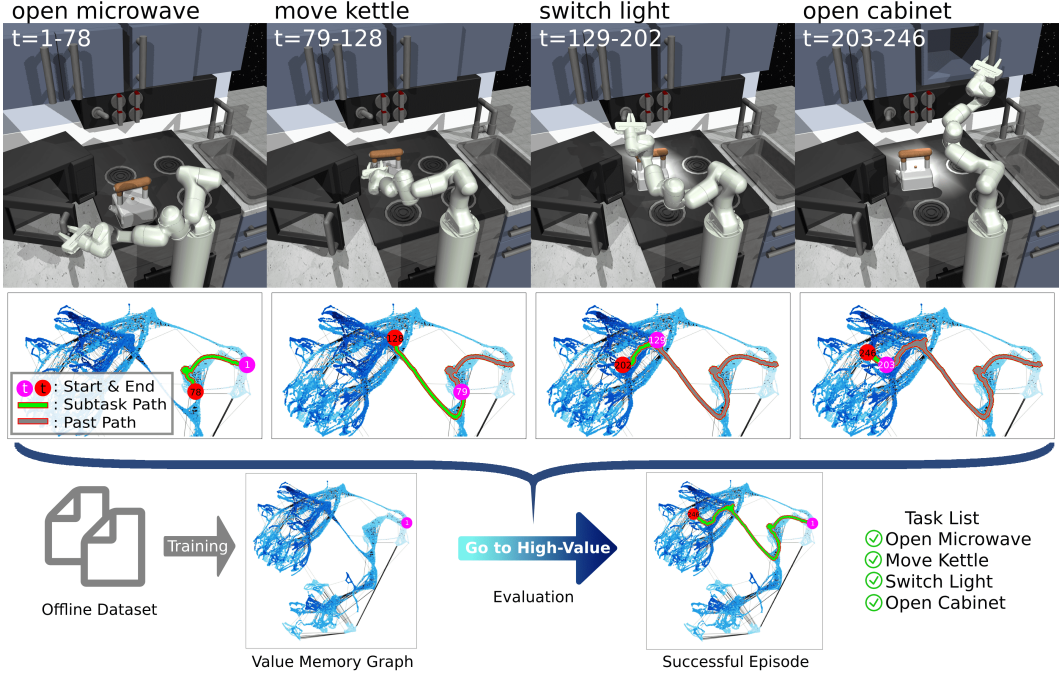


Figure 1: Demonstration of a successful episode where a robot trained in the dataset “kitchen-partial” accomplishes 4 subtasks in sequence guided by VMG. Vertex values are shown via color shade. By moving to the high-value future region (darker blue) on the graph, VMG provides good future states to guide a goal-conditioned policy so it can maximize episode rewards and finish the task.

Inspired by the success of graph-structured world models in the goal-conditioned setting and the biological evidence of cognitive maps that represent task spaces (e.g., [2, 30]), we introduce **Value Memory Graph (VMG)**, a graph-structured world model in offline reinforcement learning guided by rewards. To construct a graph from a dataset, we introduce a contrastive learning method to learn a metric space where the distance reflects the reachability among states. Then, all the original episodes are mapped into chains in the metric space and further connected into a directed graph. Based on the graph, we build a Markov decision process (MDP) as an abstract of the original environment, where vertices and edges are viewed as states and actions in the new MDP. The MDP rewards of each vertex transition are defined from the original rewards in the environment. Compared to the original continuous environment, VMG has small and discrete state and action spaces, which makes classical RL algorithms like value iteration [33] directly applicable to calculate the value of each vertex in seconds without training a neural network. Unlike previous graph-structured world model methods that require externally given targets, VMG knows what high-value states are and can provide desired targets by itself. VMG can be used to guide a low-level goal-conditioned policy trained via supervised learning (e.g., [6]). To maximize the episode return, agents select desired future states with high values in VMG to guide a goal-conditioned policy as shown in Fig.1. Our contribution can be summarized as follows:

- We introduce **Value Memory Graph (VMG)**, a graph-structured world model trained via contrastive learning in the reward-guided offline reinforcement learning setting. VMG represents the original environments as a graph-based MDP with small and discrete action and state spaces.
- We design a novel VMG-based method that guides a goal-conditioned policy to maximize episode returns in environments by providing high-value future states as goals reasoned from value iteration and graph search on VMG.
- VMG is evaluated on the offline RL benchmark D4RL and can outperform several state-of-the-art methods in many datasets where long horizon reasoning ability is required.

## 2 Related Work

**Model-based Reinforcement Learning** Recent research in model-based reinforcement learning (MBRL) has shown a significant advantage [12, 16, 13, 35, 40] in sample efficiency over model-free reinforcement learning. There are several ways to utilize the world model. For example, Dyna-style methods like [24, 16, 28, 42] use world models to augment the training data. MCTS-based methods like [35, 40, 1] plan in the world model using Monte Carlo tree search to find the best action. Other methods like [4, 13, 14] utilize the differentiability of the world model to train the policy. In contrast, our world model VMG is used to provide high-value future states that guide low-level goal-conditioned policy to maximize the episode return. World models in most previous methods are trained to approximate the environment transition. In contrast, VMG creates a graph-based MDP as an abstract of the environment and predicts the future by retrieving memory. This helps facilitate the long horizon reasoning in classical world models as all the predictions are based on actual experience no matter how long the reasoning horizon is.

**Planning as Graph Search** Recent works like [34, 8, 15, 26, 39, 7, 43] search on learned landmarks or graphs that represent the environment to improve the performance in tasks where long-horizon reasoning is crucial in a goal-conditioned setting. These methods are designed to reach given targets. It is unclear how they can be applied to a classical RL setting where agents need to maximize episode returns without given target states. To overcome this limitation, we design a Markov decision process (MDP) based on the graph with rewards defined on graph edges. Therefore, we can reason values of graph vertices and provide the high-value target by itself to guide agents and maximize episode returns in the traditional reward-guided reinforcement setting.

**Offline Reinforcement Learning** One crucial problem in offline reinforcement learning is how to avoid out-of-the-training-distribution (OOD) actions and states that decrease the performance in evaluation [10, 22, 25]. Recent works like [38, 10, 22, 31, 37, 32] directly penalizing the mismatch between the trained policy and the behavior policy via an explicit density model or via divergence. Another methods like [23, 20, 21] constrains the training via penalizing the Q function. Model-based reinforcement learning methods like [42, 41, 18] constrains the policy to the region of the world model that is close to the training data. Compare to previous methods, we use a goal-conditioned policy that controls agents to reach short-future targets states seen during training. Therefore, agents stay close to seen states without above mentioned offline RL methods. Recent works like [6, 3] show that conditioned imitation learning or RL via supervised learning (RvS) methods can work effectively in offline RL settings. Our method can be viewed as a combination of RvS and model-based RL: VMG provides high-value goal states to the goal-conditioned policy trained via supervised learning to maximize episode returns in the environment.

## 3 Value Memory Graph

Our world model Value Memory Graph (VMG) is a graph-structured Markov decision process as a highly-simplified version of the original environment. Agents can easily reason and plan on VMG to foresee the high-value future states for a goal-conditioned policy to maximize the episode return. To build VMG, we first learn a metric space that measures the reachability among states. Then, a graph is built in the metric space from the dataset as the backbone of VMG. In the end, a Markov decision process is defined on the graph as an abstract of the environment for reasoning and planning.

### 3.1 Metric Space for Value Memory Graph

VMG is built in a metric space where the L2 distance represents whether one state can be reached from another state in a few timesteps. The embedding in the metric space is based on a contrastive-learning mechanism demonstrated in Fig.2a. We have 2 neural networks: a state encoder  $Enc_s$  that maps the original state  $s$  to a state feature  $f_s$  in the metric space, and a action encoder  $Enc_a$  that maps the original action  $a$  to a transition  $\Delta f_{s,a}$  in the metric space conditioned on the current state feature  $f_s$ . Given a transition triple  $(s, a, s')$ , we add the transition  $\Delta f_{s,a}$  to the state feature  $f_s$  as the prediction of the next state feature  $\tilde{f}_{s'} = f_s + \Delta f_{s,a}$ . The prediction is encouraged to be close to the ground truth  $f_{s'}$ . In addition, we penalize the prediction  $\tilde{f}_{s'}$  if it is too close to other unrelated state features.

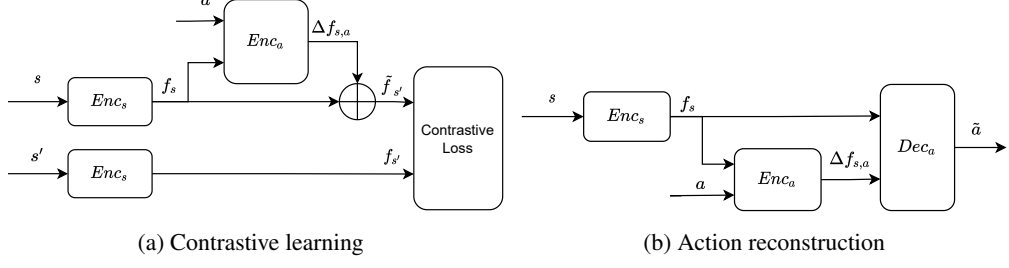


Figure 2: The training pipeline of the state encoder  $Enc_s$  and the action encoder  $Enc_a$  to build the memory map.  $Enc_s$  converts original states  $s$  into points in the memory map.  $Enc_a$  maps actions  $a$  as transitions in the memory map.

Therefore, we use the following learning objective to train  $Enc_s$  and  $Enc_a$ :

$$L_{\text{contrast}} = D^2(\tilde{f}_{s'}, f_{s'}) + \frac{1}{N} \sum \max(m - D^2(\tilde{f}_{s'}, f_{s_{\text{neg},n}}), 0) \quad (1)$$

Here,  $D(\cdot, \cdot)$  denotes the L2 distance.  $s_{\text{neg},n}$  denotes the  $n$ -th negative state. Given a batch of transition triples  $(s_i, a_i, s'_i)$  randomly sampled from the training set and a fixed margin distance  $m$ , we use all the other next states  $s'_{j|j \neq i}$  as the negative states for  $s_i$  and encourage  $\tilde{f}_{s'_i}$  to be at least  $m$  away from negative states in the metric space. In addition, we use an action decoder  $Dec_a$  to reconstruct the action from the transition  $\Delta f_{s,a}$  conditioned on the state feature  $f_s$  to extract action information better as shown in Fig.2b. Besides, we penalize the length of the transition when it is larger than the margin  $m$  to encourage adjacent states to be close in the metric space. Therefore, we have the additional action loss  $L_a$  shown below.  $L_{\text{metric}}$  is the total training loss to learn the metric space.

$$L_a = D^2(\tilde{a}, a) + \max(\|\Delta f_{s,a}\|_2, m) \quad (2)$$

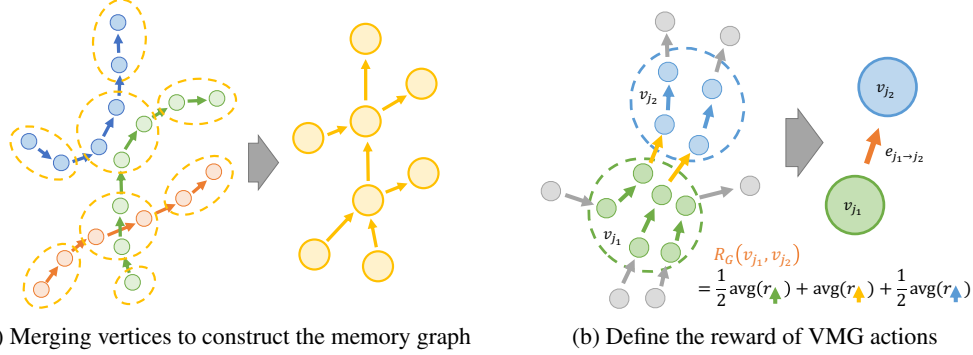
$$L_{\text{metric}} = L_{\text{contrast}} + L_a \quad (3)$$

### 3.2 Construct the Graph in VMG

To construct the graph in VMG, we first map all the episodes in the training data to the metric space as directed chains. Then, these episode chains are combined into a graph with a reduced number of state features. This is done by merging similar state features into a vertex based on the distance in the metric space. The overall algorithm are visualized in Fig.3a and can be found in the appendix. Given a distance threshold  $\gamma_m$ , a vertex set  $\mathcal{V}$ , and a checking state  $s_i$ , we check whether the minimal distance in the metric space from the existing vertices to the checking state  $s_i$  is smaller than  $\gamma_m$ . If not or if the vertex set is empty, we set the checking state  $s_i$  as a new vertex  $v_j$  and add it to  $\mathcal{V}$ . This process is repeated over the whole dataset. After the vertex set  $\mathcal{V}$  is constructed, each state  $s_i$  can be classified into a vertex  $v_j$  of which the distance in the metric space is smaller than  $\gamma_m$ . In the training set, each state transition  $(s_i, a_i, s'_i)$  represents a directed connection from  $s_i$  to  $s'_i$ . Therefore, we create the graph directed edges from the original transitions. For any vertices  $v_{j_1}, v_{j_2}$  in  $\mathcal{V}$ , if there exist a transition  $(s_i, a_i, s'_i)$  where  $s_i$  and  $s'_i$  can be classified into  $v_{j_1}$  and  $v_{j_2}$ , respectively, we add a directed edge  $e_{j_1 \rightarrow j_2}$  from  $v_{j_1}$  to  $v_{j_2}$ . Note that we don't take self connections into account. More details about graph construction can be found in the appendix.

### 3.3 Define a Graph-Based MDP

VMG is a Markov decision process (MDP)  $(\mathcal{S}_G, \mathcal{A}_G, P_G, R_G)$  defined on the graph.  $\mathcal{S}_G, \mathcal{A}_G, P_G, R_G$  denotes the state set, the action set, the state transition probability, and the reward of this new MDP, respectively. Based on the graph, each vertex in the graph is viewed as a state in the MDP. Besides, we view each directed connection  $e_{j_1 \rightarrow j_2}$  starting from a vertex  $v_{j_1}$  as an available action in  $v_{j_1}$ . Therefore, the MDP state-set  $\mathcal{S}_G$  equals the graph vertex set  $\mathcal{V}$  and the MDP action set is the graph edge set  $\mathcal{E}$ . For the MDP state transition probability  $P_G$  from  $v_{j_1}$  to  $v_{j_2}$ , we



(a) Merging vertices to construct the memory graph      (b) Define the reward of VMG actions

Figure 3: Create a graph and define rewards in VMG. In Fig.3a, Three episodes are mapped as three chains in the metric space colored differently. We merge nodes that are close to each other together and combine these chains into a directed graph. In Fig.3b, the VMG reward  $R_G(v_{j_1}, v_{j_2})$  of the action from the green vertex  $v_{j_1}$  to the blue vertex  $v_{j_2}$  is defined as the average over rewards in the original episodes.

define it as 1 if the corresponding edge exists in  $\mathcal{E}$  otherwise 0. Therefore,

$$P_G(v_{j_2}|v_{j_1}, e_{j_1 \rightarrow j_2}) = \begin{cases} 1 & \text{if } e_{j_1 \rightarrow j_2} \in \mathcal{E} \\ 0 & \text{otherwise} \end{cases} \quad (4)$$

We define the MDP reward of each possible state transition  $e_{j_1 \rightarrow j_2}$  as the average original reward from states classified to  $v_{j_1}$  to states classified to  $v_{j_2}$  in the original training set  $\mathcal{D}$  plus a “internal reward”. The internal reward are from the original transitions that are inside  $v_{j_1}$  or  $v_{j_2}$  after state merging. In detail,

$$R_{j_1 \rightarrow j_2} = \text{avg}\{r_i | \forall s_i \text{ classified to } v_{j_1}, s'_i \text{ classified to } v_{j_2}, (s_i, a_i, r_i, s'_i) \in \mathcal{D}\} \quad (5)$$

$$R_G(v_{j_1}, v_{j_2}) = \begin{cases} \frac{1}{2}R_{j_1 \rightarrow j_1} + R_{j_1 \rightarrow j_2} + \frac{1}{2}R_{j_2 \rightarrow j_2} & \text{if } e_{j_1 \rightarrow j_2} \in \mathcal{E} \\ \text{Not defined} & \text{otherwise} \end{cases} \quad (6)$$

Note that the rewards of MDP transitions outside of  $\mathcal{E}$  are not defined, as these transitions will not happen according to Eq.4. For internal rewards of the transition  $(s_i, s'_i)$  of which both the source state  $s_i$  and the target state  $s'_i$  are classified to the same vertex, we split the reward into two and allocate them to both incoming and outgoing edges, respectively. This is shown as  $\frac{1}{2}R_{j_1 \rightarrow j_1}$  and  $\frac{1}{2}R_{j_2 \rightarrow j_2}$  in Eq.6. Now we have a well-defined MDP on the graph. This MDP serves as our world model VMG. As it is discrete and finite, we can use value iteration [33] to compute the value  $V(v_j)$  of each vertex  $v_j$  in seconds without learning a neural-network-based Q function from the data.

### 3.4 Guide the Policy

With the help of VMG, agents can now foresee different futures and their corresponding values. In case we have a low-level goal-conditioned policy  $f_\pi(s, s_g)$  that is trained to reach a target  $s_g$  in the short future from the state  $s$ , VMG can provide high-value future states as the target to guide this policy. Such a policy can be trained via supervised learning using the training dataset via regressing the action given the current state and a future state [6, 5, 11]. Details of our policy training can be found in the appendix.

To guide the goal-conditioned policy, given the current state  $s_c$  in the environment, we first find the closest vertex  $v_c$  on VMG. Starting from  $v_c$ , we search for  $N_s$  future steps on VMG to find the future vertex  $v^*$  with the best value. To maximize the episode return, the agent should go towards  $v^*$  at the current step. However,  $v^*$  might be in the long future which requires dozens of steps to reach. As the policy is trained to reach the short future, we plan a weighted shortest path  $\mathcal{P}$  from  $v_c$  to  $v^*$  on the graph and select the  $N_{sg}$ -th vertex  $v_{sg}$  in the path  $\mathcal{P}$  as a subtarget. At the end, the action to execute is computed as  $a_c = f_\pi(s_c, v_{sg})$ . The weights used to plan the path  $\mathcal{P}$  are based on rewards. For each edge  $e_{j_1 \rightarrow j_2}$ , we define the edge weight  $w_{j_1 \rightarrow j_2}$  as the gap between the maximal MDP reward and the edge reward and denote the weight set as  $\mathcal{W}$ .  $w_{j_1 \rightarrow j_2} = \max\{R_G(v_{j_3}, v_{j_4}) | \forall e_{j_3 \rightarrow j_4} \in \mathcal{E}\} - R_G(v_{j_1}, v_{j_2})$ . In this case, we obtain a path that is

both short and high-rewarded. The detailed algorithm can be found in the appendix. Note that we don't apply additional regularization on the policy or world model training to avoid OOD actions, unlike many previous offline RL methods. This is because our agent is controlled to go to target states in the close future seen in the training set when execution. Therefore, the agent is encouraged to stay close to the training distribution by nature.

## 4 Experiments

### 4.1 Performance on Offline RL Benchmarks

**Test Benchmark** We evaluate VMG on the widely used offline reinforcement learning benchmark D4RL [9]. In detail, we test VMG on three domains: Kitchen, AntMaze, and Adorit. In Kitchen, we have a robot arm in a virtual kitchen. It needs to finish four subtasks in an episode. D4RL provides three different datasets in Kitchen: kitchen-complete, kitchen-partial, and kitchen-mixed. In AntMaze, a robot ant needs to go through a maze and reaches a target location. D4RL provides three mazes of different sizes. Each of them contains two datasets. In Adroit, policies control a robot hand to finish tasks like rotating a pen or opening a door. For evaluation, D4RL normalizes all the performance of different tasks to a range of 0-100, where 100 represents the performance of an “expert” policy. More benchmark details can be found in D4RL [9] and the appendix.

**Baselines** We mainly compare our method with two state-of-the-art methods CQL [23] and IQL [21] in all the above-mentioned datasets. Both CQL and IQL are based on Q-learning with constraints on the Q function to alleviate the OOD action issue in the offline setting. In addition, we also report the performance of BRAC-p [38], BEAR [22], DT [3], and AWAC [31] in the datasets they used. Performance of behavior cloning (BC) is from [21].

**Hyperparameters** In all the experiments, the dimension of metric space is set to 10. The margin  $m$  in Eq.1 and 2 is 1. The distance threshold  $\gamma_m$  is set to 0.5, 0.8, and 0.3 in Kitchen, AntMaze, and Adorit, separately. We use Adam optimizer [19] with a learning rate  $10^{-3}$  and train the model for 800 epochs with batch size 100. We train VMG for 800 epochs and select the best-performed checkpoint. More details about the hyperparameters and experiment settings are in the appendix.

**Performance** Experimental results are shown in Tab.1. VMG's scores are averaged over three individually trained models and over 100 individually evaluated episodes in the environment. In general, VMG outperforms baseline methods in Kitchen and AntMaze and shows competitive performance in Adroit. Long-horizon reasoning ability in Kitchen and AntMaze domains is required as the rewards in both domains are sparse, and the agent needs to plan over a long time before getting reward signals. Baseline methods learn a policy mapping states to actions directly and hope to obtain this ability during training. In contrast, VMG obtains the long-horizon reasoning explicitly from planning on the value memory graph. Therefore, VMG is by nature more suitable for such domains and can perform better. Adroit is the most challenging domain for all the methods in D4RL with a high-dimensional action space. VMG still shows competitive performance in Adroit compared to baselines. Experiments suggest that VMG provides a practical design of goal-conditioned reinforcement learning to work in a reward-guided setting. In tasks where the long-horizon reasoning ability is required, VMG can lead to better performance.

### 4.2 Understanding Value Memory Graph

To analyze whether VMG can understand and represent the structure of the task space correctly, we visualize an environment, the corresponding VMG, and their relationship in Fig.4. We study the task “antmaze-large-diverse” shown in Fig.4a as the state space of navigation tasks is easy to visualize and understand. The target location where the agent will receive a positive reward is denoted by the red circle. A successful trajectory is plotted as the green path. To visualize VMG, all the state features  $f_s$  are reduced to two dimensions via UMAP [29] and used as the coordinate to plot corresponding vertices as shown in Fig.4b. The vertex values are denoted by color shades. Vertices with darker blue have higher values. As shown in Fig.4b, VMG allocates high values to vertices that are close to the target location and low values to far away vertices. Besides, VMG shows a similar topology to the maze. This is further visualized in Fig.4c where graph vertices are mapped to the corresponding

Table 1: Experimental results on domains Kitchen, AntMaze, and Adroit from D4RL benchmark. VMG outperforms baselines in Kitchen and AntMaze where only sparse rewards are provided and achieve comparable performance in Adroit. Results and the standard deviation are calculated over 3 trained models.

Dataset	BC	BRAC-p	BEAR	DT	AWAC	CQL	IQL	VMG
kitchen-complete	65.0	0.0	0.0	-	-	43.8	62.5	<b>73.0</b> $\pm$ 6.7
kitchen-partial	38.0	0.0	0.0	-	-	49.8	46.3	<b>68.8</b> $\pm$ 11.9
kitchen-mixed	<b>51.5</b>	0.0	0.0	-	-	51.0	51.0	50.6 $\pm$ 4.1
<b>kitchen-total</b>	154.5	0.0	0.0	-	-	144.6	159.8	<b>192.4</b>
antmaze-umaze	54.6	-	-	59.2	56.7	74.0	87.5	<b>93.7</b> $\pm$ 2.3
antmaze-umaze-diverse	45.6	-	-	53.0	49.3	84.0	62.2	<b>94.0</b> $\pm$ 2.0
antmaze-medium-play	0.0	-	-	0.0	0.0	61.2	71.2	<b>82.7</b> $\pm$ 3.1
antmaze-medium-diverse	0.0	-	-	0.0	0.7	53.7	70.0	<b>84.3</b> $\pm$ 2.1
antmaze-large-play	0.0	-	-	0.0	0.0	15.8	39.6	<b>67.3</b> $\pm$ 3.2
antmaze-large-diverse	0.0	-	-	0.0	1.0	14.9	47.5	<b>74.3</b> $\pm$ 3.1
<b>antmaze-total</b>	100.2	-	-	112.2	107.7	303.6	378.0	<b>496.3</b>
pen-human	63.9	8.1	-1.0	-	-	37.5	<b>71.5</b>	<b>70.7</b> $\pm$ 5.2
pen-cloned	37	1.6	26.5	-	-	39.2	37.3	<b>58.2</b> $\pm$ 1.6
hammer-human	1.2	0.3	0.3	-	-	<b>4.4</b>	1.4	<b>4.1</b> $\pm$ 1.2
hammer-cloned	0.6	0.3	0.3	-	-	<b>2.1</b>	<b>2.1</b>	<b>2.2</b> $\pm$ 1.4
door-human	2	-0.3	-0.3	-	-	<b>9.9</b>	4.3	1.5 $\pm$ 0.5
door-cloned	0.0	-0.1	-0.1	-	-	0.4	1.6	<b>2.2</b> $\pm$ 0.7
<b>adroit-total</b>	104.7	9.9	25.7	-	-	93.5	118.2	<b>138.9</b>
<b>kitchen+antmaze+adroit</b>	359.4	-	-	-	-	541.7	656.0	<b>827.6</b>

maze locations to show their relationship. Our analysis suggests that VMG can learn a meaningful representation of the task. VMG is shown Another VMG visualization in the more complicated task “pen-human” is shown in Fig.5 and and more visualizations can be found in the appendix.

### 4.3 Reproducing Skills Without Rewards in Training Set

In traditional reward-guided offline RL methods, policies are trained to master skills that can maximize the accumulated return. In case there are other skills in the training set that the reward engineering doesn’t focus on, traditional reward-guided offline RL methods will simply ignore these

Table 2: The success rate of skills without rewards in the training set. Our model can perform these skills after recalculating the vertex values without model retraining.

Model	Bottom Burner	Top Burner	Hinge Cabinet
VMG (No Revalue)	0.7	3.7	0.0
VMG (Revalue)	<b>69.7</b>	<b>88.3</b>	7.3

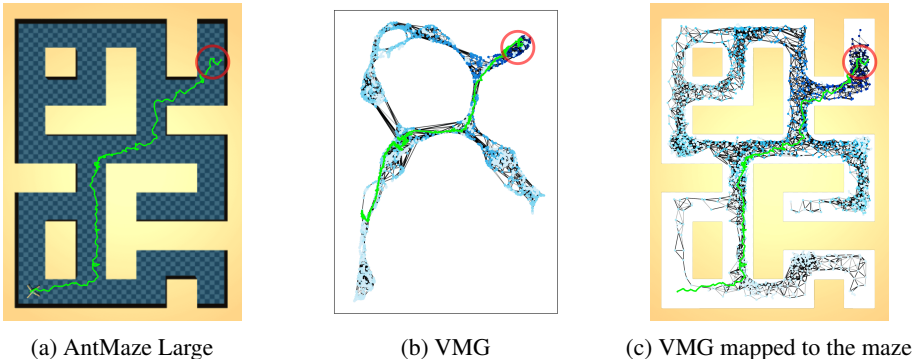


Figure 4: An example of the memory graph learned from the dataset ‘antmaze-large-diverse’. Fig.4a shows the environment with the target location denoted as a green pentagram. The memory graph is visualized via UMAP in Fig.4b. Vertex values are represented by color shades. Higher values are in darker blue. The memory graph allocates a high value to vertices that are close to the target. In Fig.4c, graph vertices are mapped to the corresponding maze locations to show the relationship.

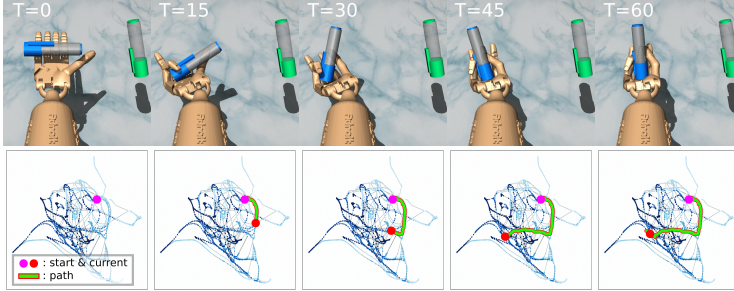


Figure 5: VMG and a successful trial in the task “pen-human”. The robot rotates the blue pen to the same orientation as the green one.

skills. As VMG remembers the training data it saw in the value memory graph, we might be able to learn these skills implicitly during training.

We design an experiment to check whether we can reproduce skills without reward signals from trained VMG models. We use the dataset “kitchen-partial” as our test platform. In “kitchen-partial”, the robot arm receives rewards when it finishes the following 4 subtasks: open a microwave, move a kettle, turn on a light, and open a slide cabinet. At the same time, there are episodes in the training set containing other skills including turning on a burner and opening a hinged cabinet without reward signals. To reproduce these skills from a trained model, we first relabel training episodes such that only the target skills have positive rewards. Then, we recalculate the vertex values by value iteration without retraining the VMG models. Experimental results in Tab.2 show that VMG learns these skills in the training time and can perform these skills after recalculating vertex values. VMG (No Revalue) denotes the models using original calculated values and VMG denotes the models after recalculation.

#### 4.4 Ablation Study

**MDP Reward** The MDP reward  $R_G(v_{j_1}, v_{j_2})$  from vertex  $v_{j_1}$  to  $v_{j_2}$  of our world model is defined as Eq.5 and Eq.6. Here we study how different designs of  $R_G(v_{j_1}, v_{j_2})$  will affect the final performance. In addition to using average in Eq.5 as the original version, here we try maximization and summation and denote them as  $R_{G,max}$  and  $R_{G,sum}$ , separately. Besides, we also try to remove the internal reward information inside a single vertex and denote this version as  $R_{G,rm}$ .  $R_{G,rm} = R_{j_1,j_2}$  if  $e_{j_1 \rightarrow j_2} \in \mathcal{E}$ . Experimental results are demonstrated in Tab.3. Results suggest that the original design of MDP rewards represent the environment rewards well and leads to the best performance.

**Distance Threshold** The distance threshold  $\gamma_m$  directly controls the “radius” of vertices and affects the size of the graph. We demonstrate how  $\gamma_m$  affects the performance in the task “kitchen-partial” in Fig.6. The dataset size of “kitchen-partial” is 137k. A larger  $\gamma_m$  can reduce the number of vertices but hurts the performance due to information loss. More results can be found in the appendix.

**State Merging Method** Vertices in VMG are merged from the original states based on a distance threshold  $\gamma_m$  as described in Sec.3.2. It is also possible to use other clustering methods to merge states. However, the dataset sizes in some tasks can be up to 1 million. Many advanced clustering methods (like BIRCH [44]) are slow (up to hours) in this case. Therefore, we compare with the classical K-means [27] implemented by Faiss [17] in the AntMaze domain and the Kitchen domain. Faiss-based K-means can be finished up to 20 seconds in our setting. Our merging method needs up to 1 minute. Experimental results are shown in Tab.4 and details can be found in the appendix. Our merging

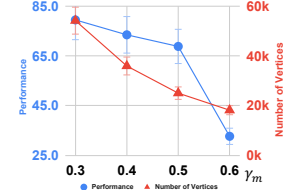


Figure 6: Influence of  $\gamma_m$  in “kitchen-partial” in performance and VMG size.

Table 3: Ablation study of reward design in VMG. The original design using average rewards over the original transitions gives us the best performance.

Model	kitchen-partial	antmaze-medium-play	pen-human
VMG $R_{G,max}$	31.5	48.3	50.8
VMG $R_{G,sum}$	50.3	56.3	66.4
VMG $R_{G,rm}$	55.0	55.0	65.2
VMG	<b>76.6</b>	<b>82.7</b>	<b>68.0</b>

Table 4: Ablation study of different state merging methods. Our original design gives us better performance.

Model	antmaze-total	kitchen-total
VMG with K-means	475.7	123.0
VMG	<b>496.3</b>	<b>192.4</b>

method also performs better than K-means in VMG. This might due to the “radius” of the vertices, since we merge states within distance  $\gamma_m$  in the metric space. In contrast, K-means cannot directly specify the cluster size and can result in clusters with different sizes. This might lead to undesired distortion in the graph and reduce the performance. More details about this experiments can be found in the appendix.

## 5 Limitations

As an attempt to combine world models and goal-conditioned reinforcement learning methods trained via supervised learning in a reward-guided reinforcement learning setting, VMG still has some limitations. For example, VMG is built directly by mapping the training dataset to the metric space. When the test environments are unseen in the training data, VMG struggles to represent the environment correctly which leads to suboptimal performance. For example, in the task “door-cloned”, the robot hand needs to open a door of which the location is randomized in all the x,y, and z directions. In case VMG meets an unseen door location in evaluation, it cannot localize the state correctly in the graph. This decrease the performance as VMG cannot provide correct guidance to the goal-conditioned policy. Besides, VMG doesn’t learn to generate new edges in the graph but only creates edges from existing transitions in the dataset. This might also hurt VMG’s generalization ability when there is not enough data provided. In addition, VMG is designed in an offline setting. Moving to the online setting requires further designs for environment exploring and dynamic graph expansion, which is non-trivial. Despite the limitations, we believe VMG shows a promising direction to improve the long-horizon reasoning ability and hope VMG can inspire more future works. For example, design a neural network that can generate, modify, and expands VMG according to the current environment to improve the generalization ability of VMG.

## 6 Conclusion

We present **Value Memory Graph** (VMG), a graph-structured world model in a reward-guided offline reinforcement learning setting. VMG is a Markov decision process defined on a directed graph trained from the offline dataset as an abstract of the environment. As VMG is finite and small, we can reason state values in VMG via value iteration instead of directly learning value functions in the original environment. VMG can provide future states with high values to guide a goal-conditioned policy trained via supervised learning. Experiments show that VMG can outperform baselines in tasks where long-horizon reasoning is needed in the widely used offline RL benchmark D4RL [9]. There are still limitations in VMG like its suboptimal generalization ability. However, we believe VMG shows a promising direction to improve the long-horizon reasoning ability and hope it can encourage more future works in this direction.

## References

- [1] Ankesh Anand, Jacob Walker, Yazhe Li, Eszter Vértes, Julian Schrittwieser, Sherjil Ozair, Théophane Weber, and Jessica B Hamrick. Procedural generalization by planning with self-supervised world models. *arXiv preprint arXiv:2111.01587*, 2021.
- [2] Dmitriy Aronov, Rhino Nevers, and David W Tank. Mapping of a non-spatial dimension by the hippocampal–entorhinal circuit. *Nature*, 543(7647):719–722, 2017.
- [3] Lili Chen, Kevin Lu, Aravind Rajeswaran, Kimin Lee, Aditya Grover, Misha Laskin, Pieter Abbeel, Aravind Srinivas, and Igor Mordatch. Decision transformer: Reinforcement learning via sequence modeling. *Advances in neural information processing systems*, 34, 2021.
- [4] Marc Deisenroth and Carl E Rasmussen. Pilco: A model-based and data-efficient approach to policy search. In *Proceedings of the 28th International Conference on machine learning (ICML-11)*, pages 465–472. Citeseer, 2011.
- [5] Yiming Ding, Carlos Florensa, Pieter Abbeel, and Mariano Phielipp. Goal-conditioned imitation learning. *Advances in neural information processing systems*, 32, 2019.
- [6] Scott Emmons, Benjamin Eysenbach, Ilya Kostrikov, and Sergey Levine. Rvs: What is essential for offline rl via supervised learning? *arXiv preprint arXiv:2112.10751*, 2021.

- [7] Scott Emmons, Ajay Jain, Misha Laskin, Thanard Kurutach, Pieter Abbeel, and Deepak Pathak. Sparse graphical memory for robust planning. *Advances in Neural Information Processing Systems*, 33:5251–5262, 2020.
- [8] Ben Eysenbach, Russ R Salakhutdinov, and Sergey Levine. Search on the replay buffer: Bridging planning and reinforcement learning. *Advances in Neural Information Processing Systems*, 32, 2019.
- [9] Justin Fu, Aviral Kumar, Ofir Nachum, George Tucker, and Sergey Levine. D4rl: Datasets for deep data-driven reinforcement learning. *arXiv preprint arXiv:2004.07219*, 2020.
- [10] Scott Fujimoto, David Meger, and Doina Precup. Off-policy deep reinforcement learning without exploration. In *International Conference on Machine Learning*, pages 2052–2062. PMLR, 2019.
- [11] Dibya Ghosh, Abhishek Gupta, Ashwin Reddy, Justin Fu, Coline Devin, Benjamin Eysenbach, and Sergey Levine. Learning to reach goals via iterated supervised learning. *arXiv preprint arXiv:1912.06088*, 2019.
- [12] David Ha and Jürgen Schmidhuber. World models. *arXiv preprint arXiv:1803.10122*, 2018.
- [13] Danijar Hafner, Timothy Lillicrap, Jimmy Ba, and Mohammad Norouzi. Dream to control: Learning behaviors by latent imagination. *arXiv preprint arXiv:1912.01603*, 2019.
- [14] Danijar Hafner, Timothy Lillicrap, Mohammad Norouzi, and Jimmy Ba. Mastering atari with discrete world models. *arXiv preprint arXiv:2010.02193*, 2020.
- [15] Zhiao Huang, Fangchen Liu, and Hao Su. Mapping state space using landmarks for universal goal reaching. *Advances in Neural Information Processing Systems*, 32, 2019.
- [16] Michael Janner, Justin Fu, Marvin Zhang, and Sergey Levine. When to trust your model: Model-based policy optimization. *Advances in Neural Information Processing Systems*, 32, 2019.
- [17] Jeff Johnson, Matthijs Douze, and Hervé Jégou. Billion-scale similarity search with GPUs. *IEEE Transactions on Big Data*, 7(3):535–547, 2019.
- [18] Rahul Kidambi, Aravind Rajeswaran, Praneeth Netrapalli, and Thorsten Joachims. Morel: Model-based offline reinforcement learning. *Advances in neural information processing systems*, 33:21810–21823, 2020.
- [19] Diederik P Kingma and Jimmy Ba. Adam: A method for stochastic optimization. *arXiv preprint arXiv:1412.6980*, 2014.
- [20] Ilya Kostrikov, Rob Fergus, Jonathan Tompson, and Ofir Nachum. Offline reinforcement learning with fisher divergence critic regularization. In *International Conference on Machine Learning*, pages 5774–5783. PMLR, 2021.
- [21] Ilya Kostrikov, Ashvin Nair, and Sergey Levine. Offline reinforcement learning with implicit q-learning. *arXiv preprint arXiv:2110.06169*, 2021.
- [22] Aviral Kumar, Justin Fu, Matthew Soh, George Tucker, and Sergey Levine. Stabilizing off-policy q-learning via bootstrapping error reduction. *Advances in Neural Information Processing Systems*, 32, 2019.
- [23] Aviral Kumar, Aurick Zhou, George Tucker, and Sergey Levine. Conservative q-learning for offline reinforcement learning. *Advances in Neural Information Processing Systems*, 33:1179–1191, 2020.
- [24] Thanard Kurutach, Ignasi Clavera, Yan Duan, Aviv Tamar, and Pieter Abbeel. Model-ensemble trust-region policy optimization. *arXiv preprint arXiv:1802.10592*, 2018.
- [25] Sergey Levine, Aviral Kumar, George Tucker, and Justin Fu. Offline reinforcement learning: Tutorial, review, and perspectives on open problems. *arXiv preprint arXiv:2005.01643*, 2020.
- [26] Kara Liu, Thanard Kurutach, Christine Tung, Pieter Abbeel, and Aviv Tamar. Hallucinative topological memory for zero-shot visual planning. In *International Conference on Machine Learning*, pages 6259–6270. PMLR, 2020.
- [27] Stuart Lloyd. Least squares quantization in pcm. *IEEE transactions on information theory*, 28(2):129–137, 1982.

[28] Yuping Luo, Huazhe Xu, Yuanzhi Li, Yuandong Tian, Trevor Darrell, and Tengyu Ma. Algorithmic framework for model-based deep reinforcement learning with theoretical guarantees. *arXiv preprint arXiv:1807.03858*, 2018.

[29] Leland McInnes, John Healy, and James Melville. Umap: Uniform manifold approximation and projection for dimension reduction. *arXiv preprint arXiv:1802.03426*, 2018.

[30] Robert M Mok and Bradley C Love. A non-spatial account of place and grid cells based on clustering models of concept learning. *Nature communications*, 10(1):1–9, 2019.

[31] Ashvin Nair, Abhishek Gupta, Murtaza Dalal, and Sergey Levine. Awac: Accelerating online reinforcement learning with offline datasets. *arXiv preprint arXiv:2006.09359*, 2020.

[32] Xue Bin Peng, Aviral Kumar, Grace Zhang, and Sergey Levine. Advantage-weighted regression: Simple and scalable off-policy reinforcement learning. *arXiv preprint arXiv:1910.00177*, 2019.

[33] Martin L Puterman. *Markov decision processes: discrete stochastic dynamic programming*. John Wiley & Sons, 2014.

[34] Nikolay Savinov, Alexey Dosovitskiy, and Vladlen Koltun. Semi-parametric topological memory for navigation. *arXiv preprint arXiv:1803.00653*, 2018.

[35] Julian Schrittwieser, Ioannis Antonoglou, Thomas Hubert, Karen Simonyan, Laurent Sifre, Simon Schmitt, Arthur Guez, Edward Lockhart, Demis Hassabis, Thore Graepel, et al. Mastering atari, go, chess and shogi by planning with a learned model. *Nature*, 588(7839):604–609, 2020.

[36] Michita Imai Takuma Seno. d3rlpy: An offline deep reinforcement library. In *NeurIPS 2021 Offline Reinforcement Learning Workshop*, December 2021.

[37] Ziyu Wang, Alexander Novikov, Konrad Zolna, Josh S Merel, Jost Tobias Springenberg, Scott E Reed, Bobak Shahriari, Noah Siegel, Caglar Gulcehre, Nicolas Heess, et al. Critic regularized regression. *Advances in Neural Information Processing Systems*, 33:7768–7778, 2020.

[38] Yifan Wu, George Tucker, and Ofir Nachum. Behavior regularized offline reinforcement learning. *arXiv preprint arXiv:1911.11361*, 2019.

[39] Ge Yang, Amy Zhang, Ari Morcos, Joelle Pineau, Pieter Abbeel, and Roberto Calandra. Plan2vec: Unsupervised representation learning by latent plans. In *Learning for Dynamics and Control*, pages 935–946. PMLR, 2020.

[40] Weirui Ye, Shaohuai Liu, Thanard Kurutach, Pieter Abbeel, and Yang Gao. Mastering atari games with limited data. *Advances in Neural Information Processing Systems*, 34, 2021.

[41] Tianhe Yu, Aviral Kumar, Rafael Rafailov, Aravind Rajeswaran, Sergey Levine, and Chelsea Finn. Combo: Conservative offline model-based policy optimization. *Advances in Neural Information Processing Systems*, 34, 2021.

[42] Tianhe Yu, Garrett Thomas, Lantao Yu, Stefano Ermon, James Y Zou, Sergey Levine, Chelsea Finn, and Tengyu Ma. Mopo: Model-based offline policy optimization. *Advances in Neural Information Processing Systems*, 33:14129–14142, 2020.

[43] Lunjun Zhang, Ge Yang, and Bradley C Stadie. World model as a graph: Learning latent landmarks for planning. In *International Conference on Machine Learning*, pages 12611–12620. PMLR, 2021.

[44] Tian Zhang, Raghu Ramakrishnan, and Miron Livny. Birch: an efficient data clustering method for very large databases. *ACM sigmod record*, 25(2):103–114, 1996.

## 7 Appendix

### Contents

<b>1</b>	<b>Introduction</b>	<b>1</b>
<b>2</b>	<b>Related Work</b>	<b>3</b>
<b>3</b>	<b>Value Memory Graph</b>	<b>3</b>
3.1	Metric Space for Value Memory Graph . . . . .	3
3.2	Construct the Graph in VMG . . . . .	4
3.3	Define a Graph-Based MDP . . . . .	4
3.4	Guide the Policy . . . . .	5
<b>4</b>	<b>Experiments</b>	<b>6</b>
4.1	Performance on Offline RL Benchmarks . . . . .	6
4.2	Understanding Value Memory Graph . . . . .	6
4.3	Reproducing Skills Without Rewards in Training Set . . . . .	7
4.4	Ablation Study . . . . .	8
<b>5</b>	<b>Limitations</b>	<b>9</b>
<b>6</b>	<b>Conclusion</b>	<b>9</b>
<b>7</b>	<b>Appendix</b>	<b>12</b>
<b>8</b>	<b>Environment details</b>	<b>13</b>
<b>9</b>	<b>Details of Policy Training</b>	<b>13</b>
<b>10</b>	<b>Algorithms</b>	<b>13</b>
<b>11</b>	<b>Architecture of Neural Networks</b>	<b>14</b>
<b>12</b>	<b>Experiment Settings and Hyperparameters</b>	<b>14</b>
<b>13</b>	<b>Methods to Alleviate Generalization Limitation</b>	<b>14</b>
<b>14</b>	<b>Ablation Studies</b>	<b>14</b>
<b>15</b>	<b>Visualization of VMG</b>	<b>15</b>
<b>16</b>	<b>Future Works</b>	<b>15</b>

## 8 Environment details

The datasets in D4RL [9] is under CC BY license and the related code is under Apache 2.0 License. We use the latest version of the datasets (v1/v0/v1 for AntMaze, Kithcen, Adroit, separately). Different versions of datasets contain exactly the same training transitions. The newer version fixes some bugs in the meta data information like the wrong termination steps. For more details about the datasets please refer to D4RL [9].

## 9 Details of Policy Training

The goal-conditioned policy is trained via supervised learning to regress the action given the current state and a target state in the short-horizon future. In detail, given a timestep  $t$  in an episode from the training set and a future horizon  $K$ , we randomly sample a step  $t + k$  from the future  $K$  steps. Then, the policy is trained to regress the action  $a_t$  at step  $t$  given the state  $s_t$  and the future state  $s_{t+k}$  as the target using Eq.7.

$$L_\pi = D^2(f_\pi(s_t, s_{t+k}), a_t) \quad (7)$$

## 10 Algorithms

The detailed algorithms of graph construction and policy execution are shown in Alg.1 and Alg.2.

---

### Algorithm 1: Graph Construction

---

**Input :** Training Set  $\mathcal{D} = \{(s_i, a_i, r_i, s'_i) | i = 1, 2, \dots, N\}$ , Empty vertices set  $\mathcal{V} = \{\}$ , Vertex index  $J = 1$ , Distance threshold  $\gamma_m$ , Empty edges set  $\mathcal{E} = \{\}$

```

1 for  $(s_i, a_i, r_i, s'_i)$  in  $\mathcal{D}$  do
2    $f_{s_i} = Enc_s(s_i)$ 
3   Compute the distance  $d_{ij}$  between  $f_{s_i}$  and  $f_{v_j}$  for every  $f_{v_j}$  in  $\mathcal{V}$ 
4   if  $\min\{d_{ij} | f_{s_j} \text{ in } \mathcal{V}\} > \gamma_m \text{ or } J = 1$  then
5      $v_J \leftarrow s_i, f_{v_J} \leftarrow f_{s_i}$ 
6      $\mathcal{V}.\text{append}((v_J, f_{v_J}))$ 
7      $J \leftarrow J + 1$ 
8   end
9 end
10 for  $(s_i, a_i, r_i, s'_i)$  in  $\mathcal{D}$  do
11   Find  $v_{j_1}, v_{j_2}$  that  $s_i$  and  $s'_i$  are classified to in  $\mathcal{V}$ , respectively
12   if  $v_{j_1} \neq v_{j_2}$  and the connection  $e_{j_1 \rightarrow j_2} \notin \mathcal{E}$  then
13      $\mathcal{E}.\text{append}(e_{j_1 \rightarrow j_2})$ 
14   end
15 end

```

---



---

### Algorithm 2: Policy Execution

---

**Input :** Current state  $s_c$ , State encoder  $Enc_s$ , Goal-conditioned policy  $f_\pi$ , Vertex and edge sets in VMG  $(\mathcal{V}, \mathcal{E})$ , Vertices value  $V$ , Edge weight  $\mathcal{W}$

```

1  $f_{s_c} = Enc_s(s_c)$ 
2  $v_c = \arg \min_{v_j | (v_j, f_j) \in \mathcal{V}} D(f_{s_c}, f_j)$ 
3 Search future horizon of  $N_s$  steps starting from  $v_c$  and select the best value vertex  $v^*$ 
4 Compute the weighted shortest path  $\mathcal{P}$  from  $v_c$  to  $v^*$  via Dijkstra
5 Select the  $N_{sg}$ -th vertex  $v_{sg}$  in  $\mathcal{P}$ 
6  $a_c = f_\pi(s_c, v_{sg})$ 

```

---

## 11 Architecture of Neural Networks

For all the networks including the state encoder  $Enc_s$ , the action encoder  $Enc_a$ , the action decoder  $Dec_a$ , and the policy  $f_\pi$ , we use a 3-layer MLP with hidden size 256 and ReLU activation functions.

## 12 Experiment Settings and Hyperparameters

Our model is trained in a single RTX Titan GPU in about 1.5 hours. We implement VMG on the top of the offline RL python package d3rlpy [36] with MIT license. In all the experiments, We use Adam optimizer [19] with a learning rate  $10^{-3}$ . Batch size is 100. Each model is trained for 800 epochs. We save models per 100 epochs and report the performance of the best one from the checkpoints saved from the 500th to the 800th epochs. The remaining hyperparameter settings can be found in Tab.5.  $N_s = \infty$  means we search the future steps till the end of the graph. For the domain Kitchen, the hyperparameters are tuned in “kitchen-partial”. For AntMaze it is “antmaze-umaze-diverse”. For Adroit, hyperparameters are tuned individually.

Table 5: Detailed Hyperparameter Setting

Dataset	$m$	$K$	$\gamma_m$	discount	$N_{sg}$	$N_s$
kitchen-complete	1	10	0.5	0.95	2	$\infty$
kitchen-partial	1	10	0.5	0.95	2	$\infty$
kitchen-mixed	1	10	0.5	0.95	2	$\infty$
antmaze-umaze	1	10	0.8	0.8	1	$\infty$
antmaze-umaze-diverse	1	10	0.8	0.8	1	$\infty$
antmaze-medium-play	1	10	0.8	0.8	1	$\infty$
antmaze-medium-diverse	1	10	0.8	0.8	1	$\infty$
antmaze-large-play	1	10	0.8	0.8	1	$\infty$
antmaze-large-diverse	1	10	0.8	0.8	1	$\infty$
pen-human	1	10	0.3	0.8	2	12
pen-cloned	1	10	0.3	0.8	2	12
hammer-human	1	10	1.0	0.8	2	12
hammer-cloned	1	10	1.0	0.8	2	12
door-human	1	10	0.3	0.8	2	12
door-cloned	1	10	0.3	0.8	2	12

## 13 Methods to Alleviate Generalization Limitation

As discussed in the limitation section, VMG doesn’t generalize well to environments that are unseen during training due to the incorrect localization of the state on the graph. This happens in the tasks “hammer-\*”, and “door-\*” in the Adroit domain where the location of the objects like the door and the nail are randomized and can be unseen in the training stage. To alleviate this issue, when retrieving the closest vertex  $v_c$  on the graph given the current state  $s_c$ , we additionally reduce the search space to vertices where the object locations are the top-100 closest to that in  $s_c$ . In addition, we remove the components in the graph in which there are no high-value vertices to avoid value-less guidance. These two methods are applied only in “hammer-\*” and “door-\*”.

## 14 Ablation Studies

**Distance Threshold** More experimental results of the distance threshold  $\gamma_m$  in the tasks “antmaze-medium-play” and “pen-cloned” can be found in Fig.7. Results suggest that the model is not so sensitive to  $\gamma_m$  if it is not too large.

**State Merging Method** Detailed results of the state merging method ablation experiment are shown in Tab.6. As K-means doesn’t have a parameter to control the size of the clusters directly, we have to search for the best number of clusters for every dataset. The number of clusters used in K-means is shown in Tab.7.

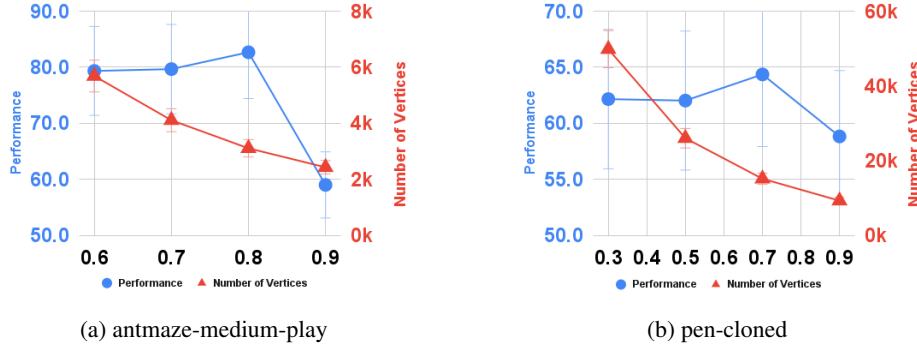


Figure 7: More results of the influence of  $\gamma_m$  in performance and VMG size

Table 6: Detailed results of different state merging ablation

Model	AntMaze						Kitchen		
	umaze	umaze-diverse	medium-play	medium-diverse	large-play	large-diverse	complete	partial	mixed
VMG with K-means	88.7	79.7	81.2	77.0	<b>72.3</b>	<b>76.3</b>	61.1	18.3	43.6
VMG	<b>93.7</b>	<b>94.0</b>	<b>82.7</b>	<b>84.3</b>	67.3	74.3	<b>73.0</b>	<b>68.8</b>	<b>50.6</b>

Table 7: Number of clusters used in K-means

AntMaze						Kitchen		
umaze	umaze-diverse	medium-play	medium-diverse	large-play	large-diverse	complete	partial	mixed
6000	2000	1000	1000	10000	10000	3000	25000	25000

## 15 Visualization of VMG

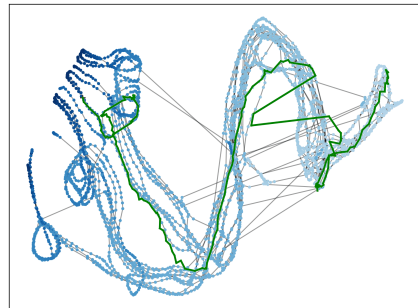
More visualization of VMG in different tasks are demonstrated in Fig.8, 9, 10, 11. An episode is denoted as a green path on the graph with a “+” sign at the end.

## 16 Future Works

There are several directions to improve VMG. Building hierarchical graphs to model different levels of environment structures might help represent the environment better. For example, if a robot needs to cook a meal, we might have a high-level graph to represent abstract tasks like washing vegetables, cutting vegetables, etc. A low-level graph can be used to guide a goal-conditioned policy. This might improve the high-level planning of the tasks. Extending VMG into the online setting is also an important future step. In online reinforcement learning, data with new information is collected throughout the training stage. Therefore, the graph needs to have a mechanism to continually expand and include the new information. Besides, exploration is a crucial component in online reinforcement learning. If we model the uncertainty of the graph, VMG can be used to guide the agent to explore regions with high uncertainty to explore more effectively. Combined with Monte Carlo tree search on VMG might also help policy explore and exploit better. In the end, improving the generalization ability of VMG is crucial. Instead of memorizing the previous experience as a static graph, designing a conditioned generative model to create a graph that adapts to the current observation like object locations might be a promising way to generalize better.



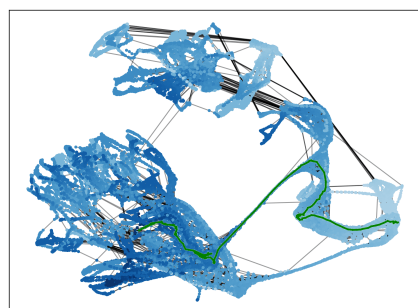
(a) kitchen-complete



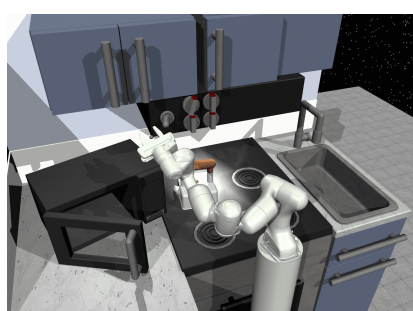
(b) VMG of kitchen-complete



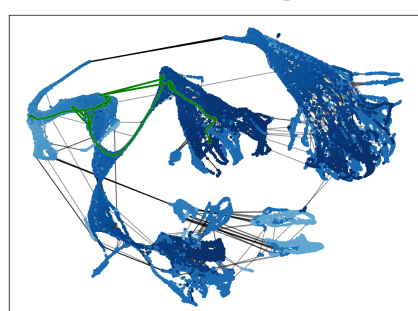
(c) kitchen-partial



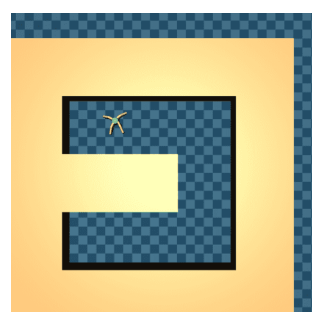
(d) VMG of kitchen-partial



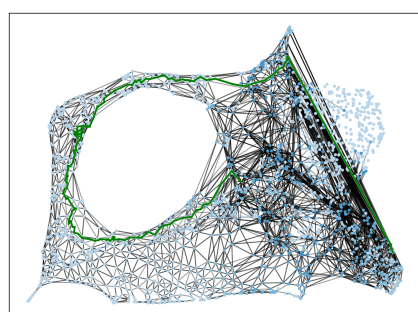
(e) kitchen-mixed



(f) VMG of kitchen-mixed

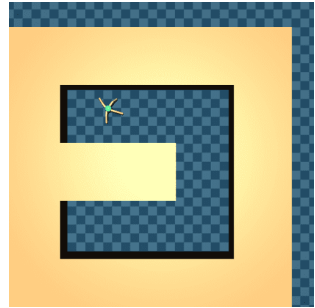


(g) antmaze-umaze

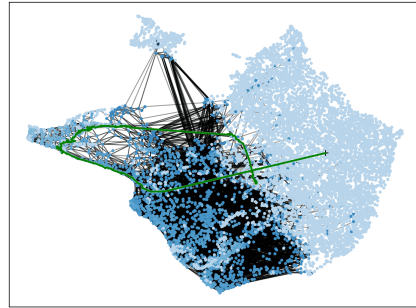


(h) VMG of antmaze-umaze

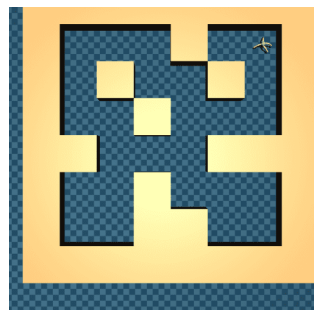
Figure 8: Visualization of VMG in different tasks



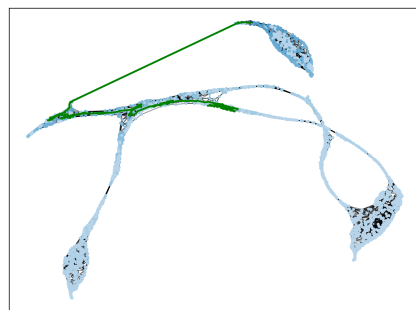
(a) antmaze-umaze-diverse



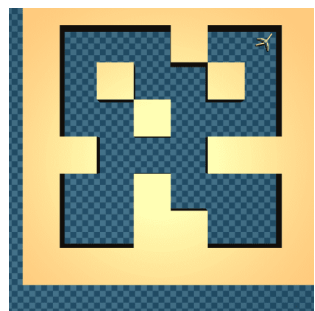
(b) VMG of antmaze-umaze-diverse



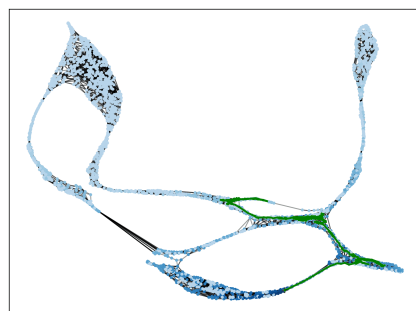
(c) antmaze-medium-play



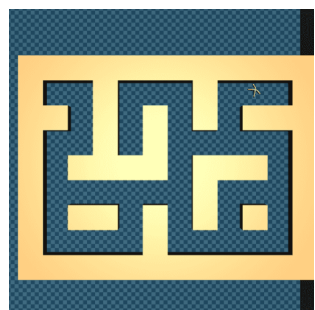
(d) VMG of antmaze-medium-play



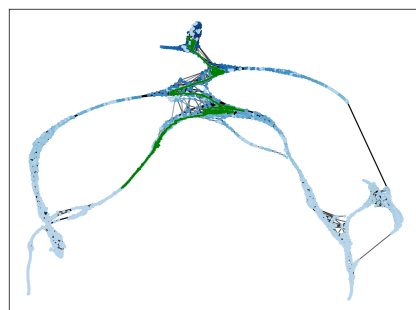
(e) antmaze-medium-diverse



(f) VMG of antmaze-medium-diverse

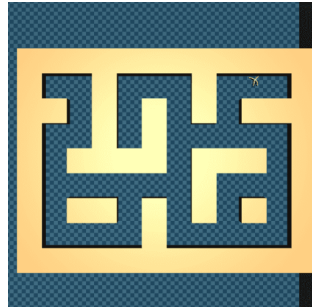


(g) antmaze-large-play

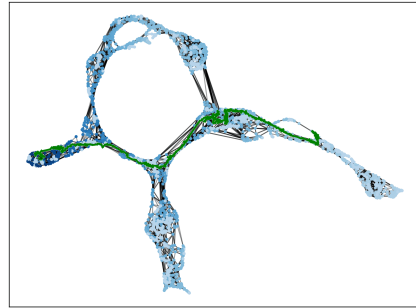


(h) VMG of antmaze-large-play

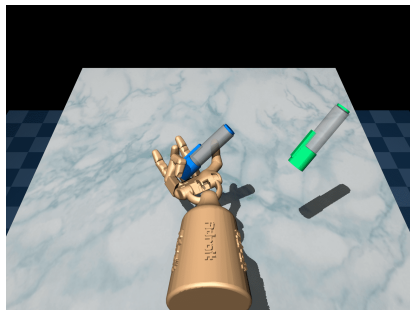
Figure 9: Visualization of VMG in different tasks



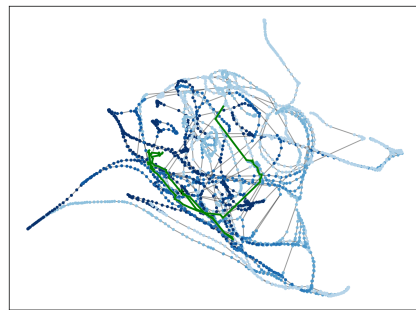
(a) antmaze-large-diverse



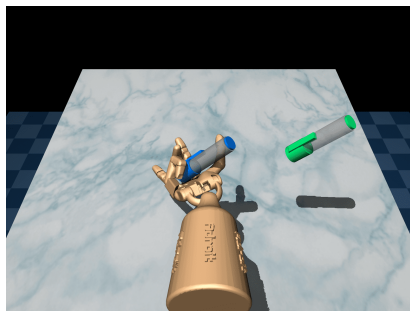
(b) VMG of antmaze-large-diverse



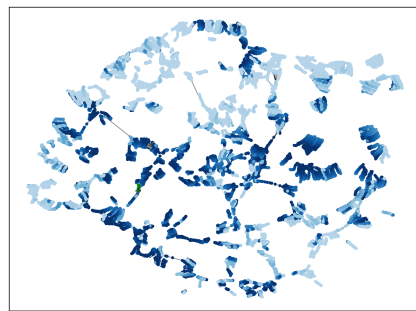
(c) pen-human



(d) VMG of pen-human



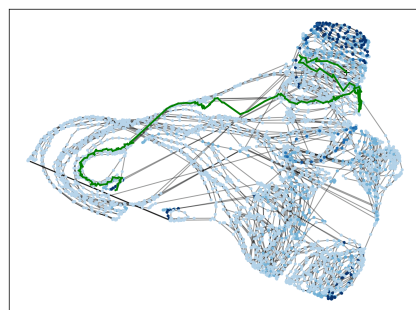
(e) pen-cloned



(f) VMG of pen-cloned

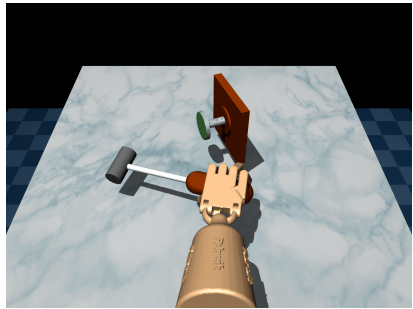


(g) hammer-human

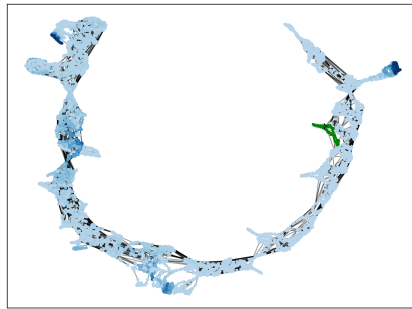


(h) VMG of hammer-human

Figure 10: Visualization of VMG in different tasks



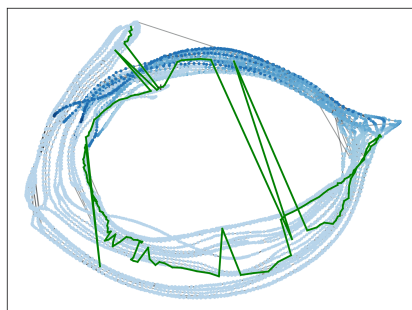
(a) hammer-cloned



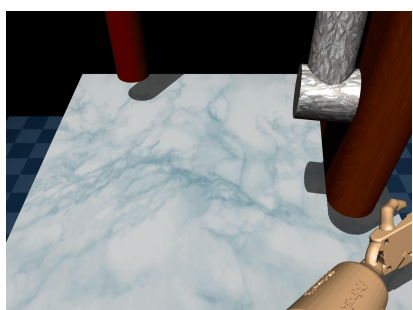
(b) VMG of hammer-cloned



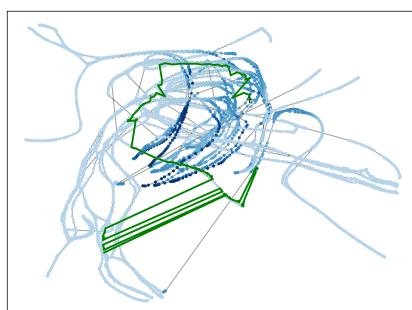
(c) door-human



(d) VMG of door-human



(e) door-graph



(f) VMG of door-graph

Figure 11: Visualization of VMG in different tasks